

TPF-5(433) Behavior of Reinforced and Unreinforced Lightweight Cellular  
Concrete (LCC) For Retaining Walls

**Interim Report on Second Unreinforced Lightweight Cellular Concrete Test**

*Prepared by*

Prof. Kyle M. Rollins

Civil & Environmental Engineering Dept.  
Brigham Young University  
430 EB, Provo, UT 84602

*Prepared for*

David Stevens, Project Manager

Research & Innovation Division  
Utah Department of Transportation  
4501 S. 2700 W.  
Salt Lake City, UT 84114



June 27, 2020

## **Background**

This test is the first test conducted as part of the TPF-5(433), but the second unreinforced lightweight cellular concrete (LCC) test performed with this test box. The first unreinforced (LCC) test was performed under a separate contract with the Utah Dept. of Transportation to the University of Utah through a sub-contract to Brigham Young University. Additional details regarding this first test are discussed subsequently.

## **Test Set-up**

Schematic plan and profile drawings for the unreinforced LCC test are shown in Fig. 1. The test box is 10 ft tall x 12 ft long x 10 ft wide. The reinforced concrete (RC) cantilever wall had a 1-foot thick slab that was six feet long and a 1-foot thick stem wall extending to a height of 10 ft. The cellular concrete had a unit weight of 27 lbs/ft<sup>3</sup> and an unconfined compressive strength (UCS) of about 100 psi at the time of the load test. The cellular concrete was placed in 2.5-foot thick lifts to a height of 10 feet behind the RC cantilever retaining wall over a four-day period (one pour per day). The three steel braced walls (shown in red) were stiff enough to constrain lateral movements to less than 0.1 inch at the maximum expected surcharge load of about 64 psi (7200 psf) based on SAP2000 analyses of the steel frame. The test box was designed so that we could apply load independently to six stiff concrete beams (2 ft wide by 10 ft long) using independently activated hydraulic jacks with load cells.

Six Geokon pressure cells were placed at approximately 1.5 ft vertical intervals on the back face of the retaining wall to monitor interface pressure on the wall during the backfill placement, curing, and surcharge loading. In addition, four hybrid pressure sensors, developed by Prof. Mark Talesnick (Technion, Haifa, Israel) were installed at depths of 2.5 ft. from the top and bottom of the cantilever wall. Two of these pressure sensors were located approximately 1.5 foot inside the LCC block, while two were located at the LCC-wall interface. Finally, 11 thin-film pressure cells developed by Sensor Products were placed at the center of the top three lifts at the LCC-MSE wall interface.

Deformation of the retaining wall, the LCC backfill and the test box was monitored using a series of string potentiometers from fill placement to failure that were connected to a data acquisition system. A digital image correlation (DIC) system was also used to monitor the deflection of the retaining wall face to create a color contour map of wall displacements. Thin electrical cables were installed at eight depths within the LCC backfill and monitored with a time-domain reflectometer (TDR) to identify potential failure plane development during surcharge loading. Finally, at the conclusion of the test, the sides of the box and the surcharge panels were removed to identify shear plane and crack patterns in the LCC.

## **Loading Procedure**

Photographs of the test box just prior to testing the RC retaining wall are provided in Fig. 2. For each test, we applied the surcharge load incrementally at 25,000 lbs to 50,000 lbs load increments or 2.75 to 5.5 psi pressure increments. For the test on the RC retaining wall, load was applied to the first three surcharge blocks (6 ft) adjacent to the retaining wall as illustrated

schematically in Fig. 3(a). For the test against the free face, with no retaining wall, load was applied to the first three surcharge blocks (6 ft) adjacent to the free face as illustrated schematically in Fig. 3(b). The load was quite uniformly distributed over the three blocks in each case, but settlement under the load could be different. Displacement of each block was monitored with three string potentiometers attached to an independent reference frame.

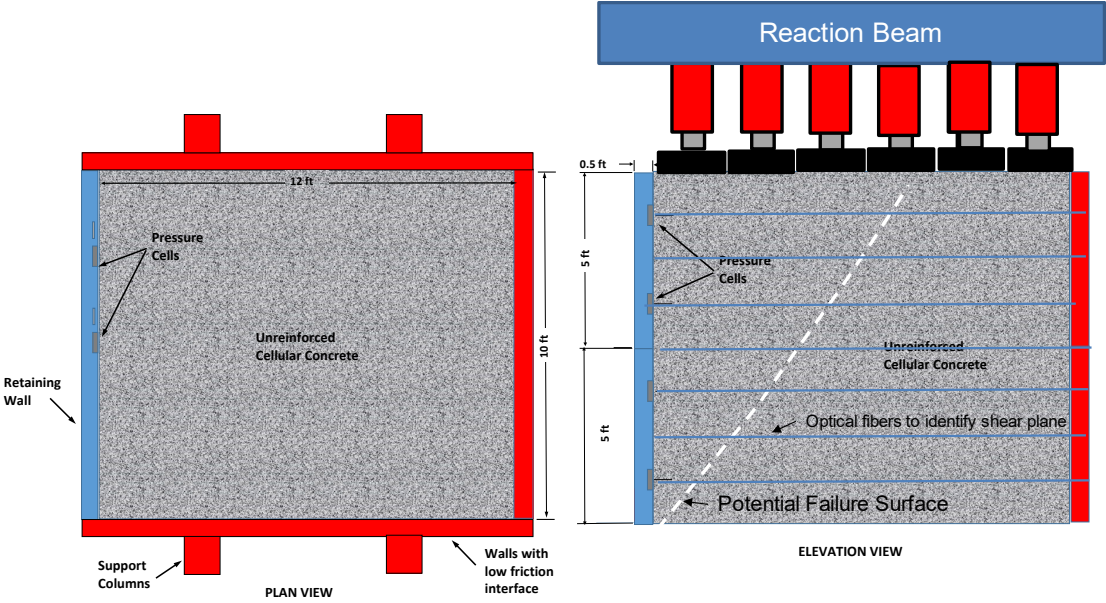


Fig. 1. Schematic plan and profile drawings of the test with unreinforced LCC behind reinforced concrete cantilever retaining wall.

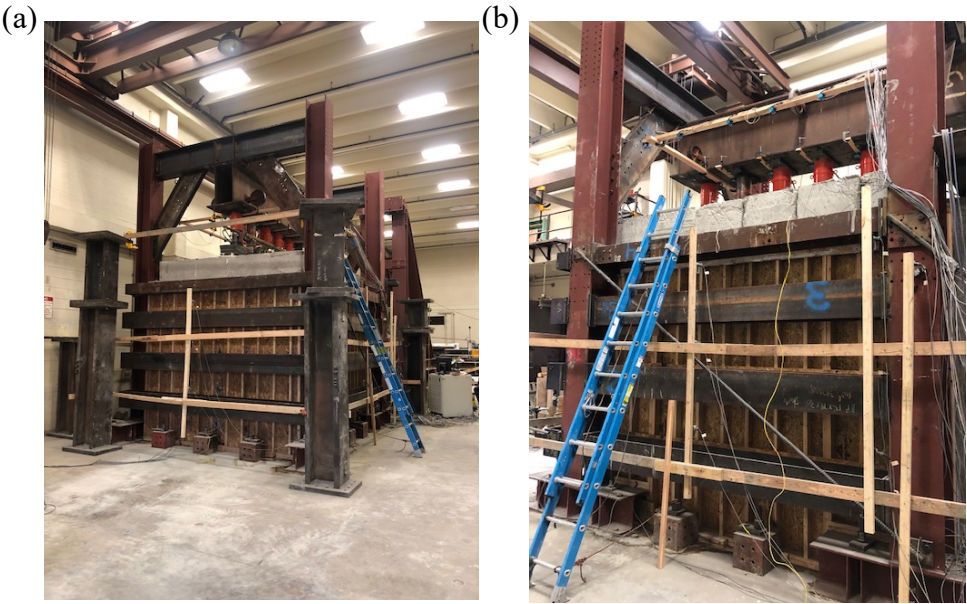
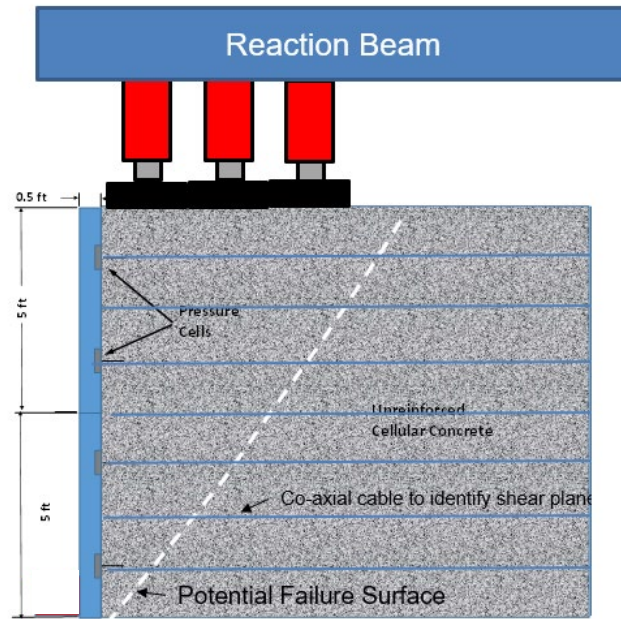


Fig. 2 Photographs showing: (a) the test box from the short side opposite from the retaining wall and (b) the test box from the long side with the concrete surcharge blocks and hydraulic jacks reacting against a longitudinal T-beam.

(a)



(b)

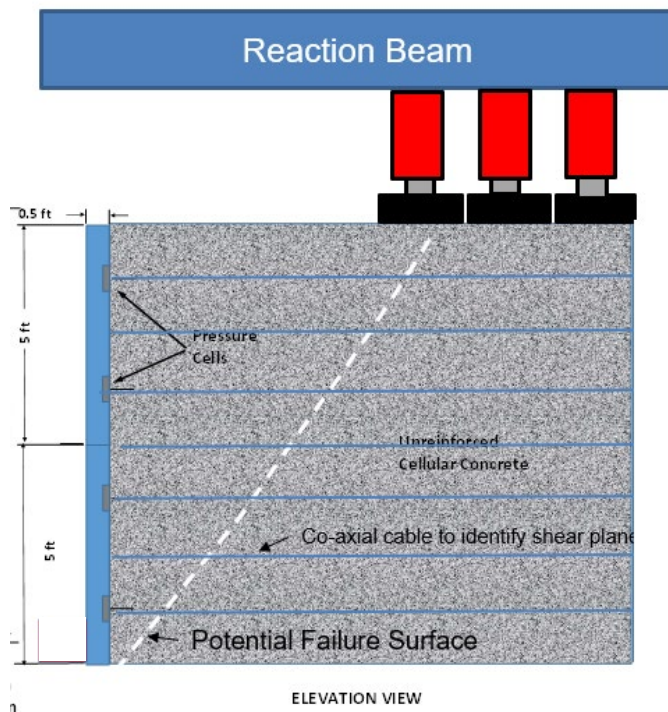


Fig. 3. Schematic drawings illustrating the surcharge load application for (a) the RC cantilever wall test and (b) the free face wall test.

## Test Results

A plot of the applied surcharge pressure versus axial displacement is provided in Fig. 4. The stiffness of the curve near the RC wall is somewhat higher than that for the free face, but the difference is not large. However, at a surcharge pressure of about 44 psi, the axial settlement near the wall increases rapidly and the surcharge pressure decreases as the LCC loses strength after reaching its peak strength. In contrast, the test near the RC wall continues to carry higher surcharge pressures up to a value of about 63 psi, where settlement increases to over 3 inches at constant pressure. Failure of the RC cantilever wall exhibits ductile behavior, while the free face does not.

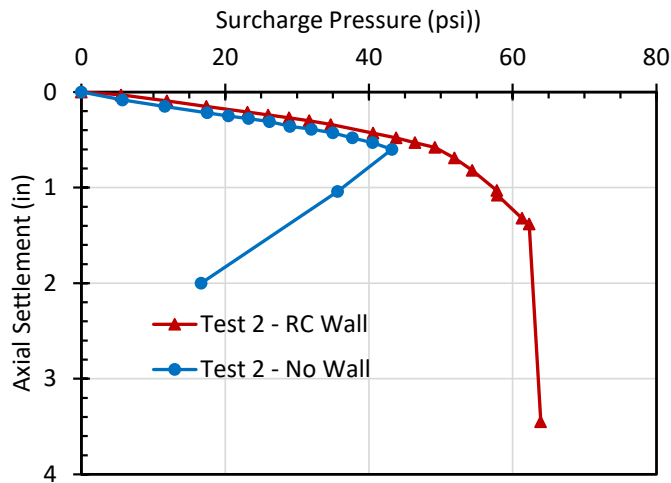


Fig. 4. Applied surcharge pressure versus axial displacement in the LCC for tests with and without RC cantilever wall.

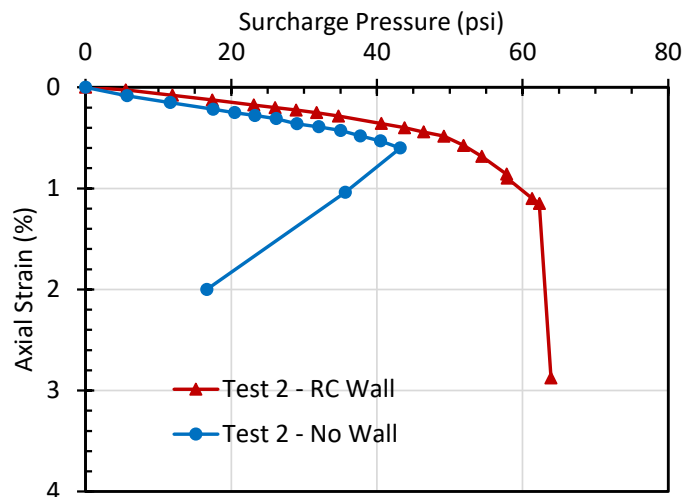


Fig. 5 Applied surcharge pressure versus axial strain in the LCC for tests with and without RC cantilever wall.

Fig. 5 shows plots of surcharge pressure vs. axial strain for both wall tests. The curves show that failure occurred at axial strains of 0.6% and 1.2% for the free face and RC wall tests, respectively.

A plot of applied surcharge pressure vs. lateral wall displacement is provided in Fig. 6 for both walls. The pressure vs. displacement curves are very similar until a pressure of 44 psi suggesting that the strength of the LCC provided most of the resistance to this point. At higher pressures, the curve for the free face experiences significant lateral displacement as surcharge pressure decreases. In contrast, the pressure vs. lateral displacement curve near the RC wall continues to show an increase in resistance that must come primarily from the strength of the retaining wall. There is a significant reduction in stiffness at a surcharge pressure of about 50 psi and failure of the retaining wall occurs at a surcharge pressure of about 63 psi when the wall begins to deform without an increase in applied pressure.

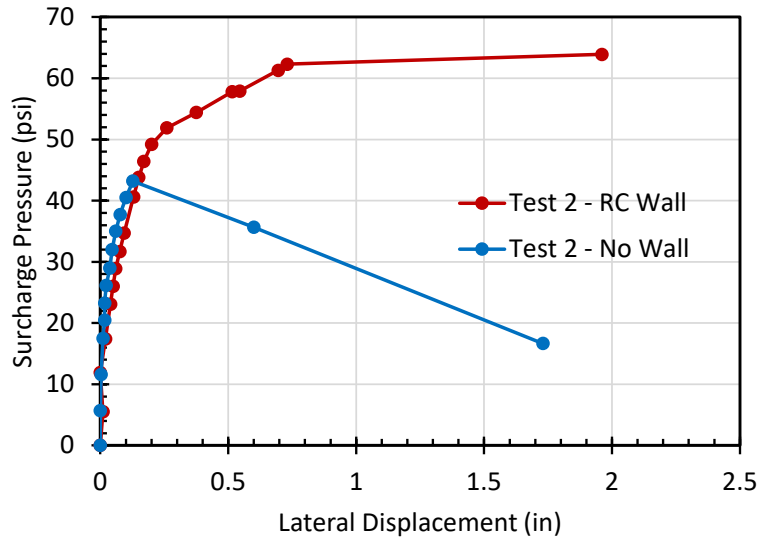


Fig. 6. Applied surcharge pressure vs. lateral wall displacement in the LCC for tests with and without RC cantilever retaining wall for unreinforced LLC test 2.

Fig. 7 provides a comparison of the surcharge pressure vs. lateral wall displacement for the first and second unreinforced LCC tests with the RC cantilever retaining wall. The unconfined compressive strength of the LCC during the first test was approximately 40 psi, relative to about 100 psi in the second test. In contrast with the second set of unreinforced LLC tests described in this report, the surcharge pressure for the first test was applied uniformly across the entire surface area of the LCC block. For the uniform pressure in test 1, the plot in Fig. 7 indicates that there was absolutely no lateral movement of the top of the wall up to a pressure of 40 psi. In an effort to induce some lateral displacement, the surcharge pressure was entirely removed, and pressure was only re-applied to the first four surcharge blocks (8 feet behind the RC wall). For this loading scheme, the wall began to move laterally beyond a pressure of 40 psi, although movements were small. It should be noted; however, that this was after the entire LCC block had already been pre-compressed to 40 psi under a

uniform pressure that could have increased strength and stiffness. Despite the higher compressive strength of the LCC for test 2 (UCS=100 psi), significantly more displacement occurred at surcharge pressures less than 40 psi than for test 1 (UCS=40 psi). In addition, failure occurred at 63 psi, which is much smaller than the compressive strength of the LCC. These results indicate that the partial loading condition, which induces a shear plane, is more critical for retaining wall performance than a uniform surface pressure over the entire surface which primarily induces compressive strain.

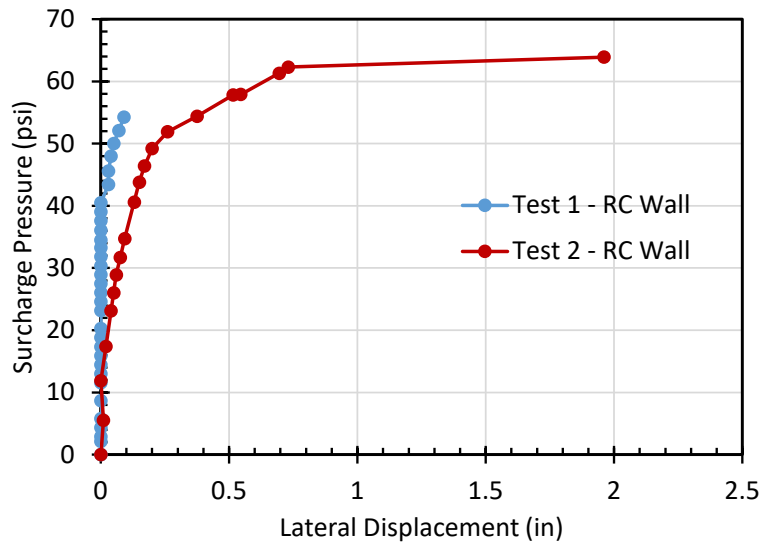


Fig. 7. Applied surcharge pressure vs. lateral wall displacement with RC cantilever retaining wall for unreinforced LCC tests 1 and 2.

Fig. 8 provides a comparison of the surcharge pressure vs. lateral wall displacement for the first and second unreinforced LCC tests adjacent to free face (no retaining wall). For these two tests the surcharge pressure was applied over an area 6 feet back from the wall face. Despite the higher compressive strength of the LCC for test 2 (UCS=100 psi), both tests reached a failure condition at about 45 psi. The lower strength LCC had a much more ductile failure than the higher strength LCC. Once again, it must be noted that prior to test 1 adjacent to the free face, the entire LCC block had already been pre-compressed to 40 psi under a uniform pressure that could have increased strength and stiffness. As a result, further comparisons are difficult to interpret.

Fig. 9 provides plots of horizontal pressure on the RC wall versus depth for selected applied surcharge pressures during loading as measured by the Geokon pressure plates. As the surcharge pressure increases, the pressure on the wall progressively increases with higher pressures developing in the top half of the wall, followed by increased pressures in the bottom half.

Recent investigations by Tiwari et al. (2018) and Black (2018) have concluded that the shear strength of LCC can be approximated using a friction angle ( $\phi$ ) of  $34^\circ$  and a cohesion ranging from 700 to 1000 (Black 2018) or 700 to 1600 psf (Tiwari et al. 2018). If this strength model

is adopted, then the horizontal pressure ( $\sigma_h$ ) versus depth on the wall due to the LCC during surcharge loading can be computed using the equation

$$\sigma_h = \gamma z K_a + q K_a - 2c K_a^{0.5} \quad (1)$$

where  $K_a = \tan^2(45 - \phi/2)$ ,  $\phi = 34^\circ$ ,  $c = 700$  to  $1000$  psf,  $\gamma = 27$  lbs/ft<sup>3</sup>,  $q$  = surcharge pressure, and  $z$  = depth below the ground surface. The range of theoretical horizontal pressures ( $c = 700$  to  $1000$  psf) on the cantilever wall computed using Equation 1 is plotted relative to the measured horizontal pressures in Fig. 9. In this case, the theoretical horizontal pressure range provides a reasonable upper boundary for the measured horizontal pressures.

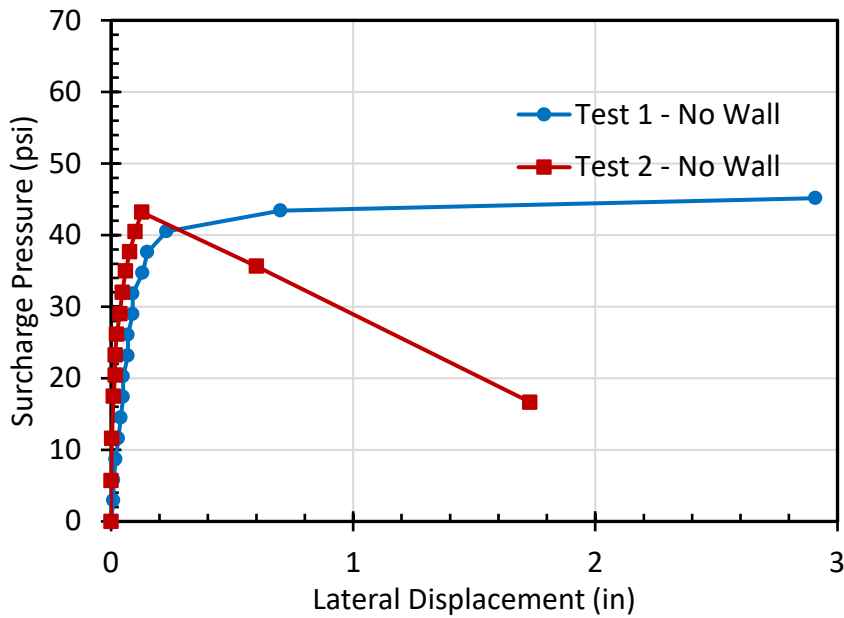


Fig. 8. Applied surcharge pressure vs. lateral wall displacement with no retaining wall (free face) for unreinforced LCC tests 1 and 2.

Based on the string potentiometer measurements on the front face of the cantilever retaining wall, horizontal wall deflection has been plotted as a function of height above the base of the wall for selected surcharge pressures in Fig. 10. The deflection curves are close to zero at the base indicating that the wall was bending, not sliding during the surcharge loading. The horizontal deflection profile is typical of what would be expected for a cantilever wall under lateral loading.

At the completion of the test, one side wall and the back wall (free face) were both removed to provide a view of the crack patterns produced by the load testing. Drones were also used to photograph the LCC block from multiple angles to produce a 3D point cloud model of the deformed geometry using structure from motion software. Fig. 11 provides a photograph from the side of the LLC block while Fig. 12 provides 3D point cloud representations of the crack patterns in the LCC block. The cracks painted in blue likely developed during loading near the RC cantilever wall, while the cracks painted in yellow likely developed during

loading near the free face with no wall. The blue cracks suggest that a nearly vertical shear plane developed at the back side of the third surcharge block (6 feet behind the wall), due to the 3 inch offset at the top of the LCC block (see Fig. 12 (b)), and propagated to a depth of about 5 feet (mid-height). The failure plane then appears to move to the base of the stem wall at an angle of  $39^\circ$  as shown in Fig. 11.

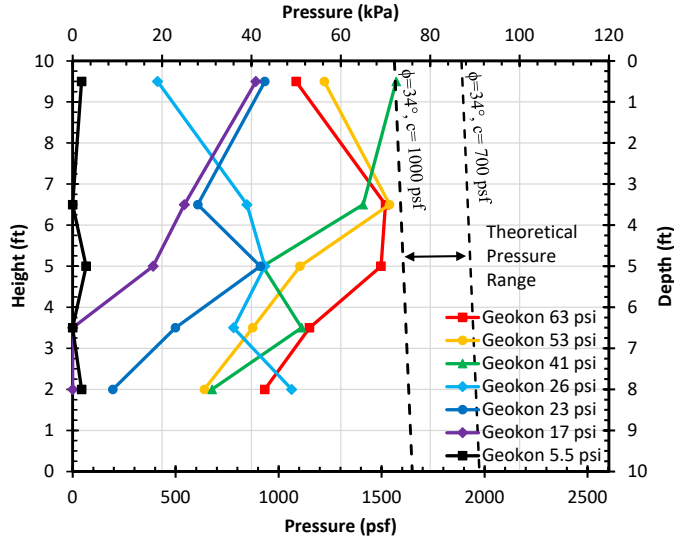


Fig. 9. Horizontal pressure on the RC wall versus depth curves for selected applied surcharge pressure values near the wall during test 2 as measured by Geokon pressure plates.

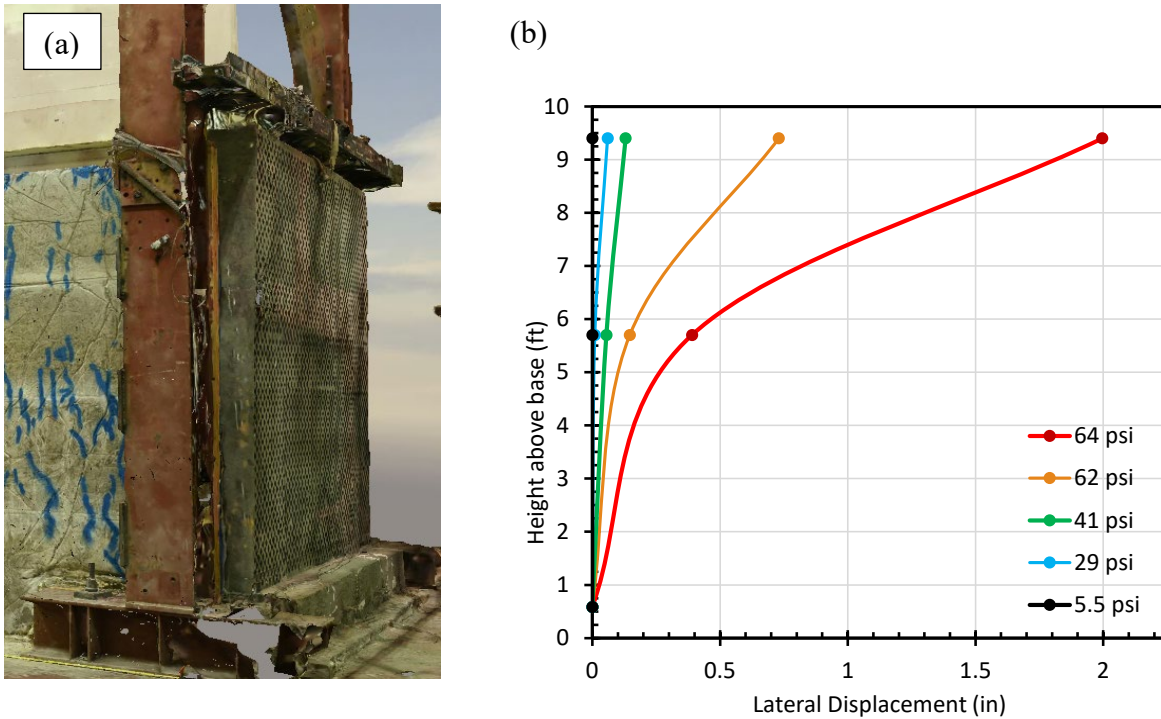


Fig. 10 (a) 3D point cloud of cantilever wall deflection at failure, and (b) measured horizontal deflection of the wall versus height above the base of the wall for selected surcharge pressures.

This failure surface is similar to what would be expected for an MSE wall where the failure wedge extends vertically downward at a distance of  $0.3H$  (3 feet) behind the wall to a depth of  $0.5H$  (5 feet) and then slopes at an angle  $45+\phi/2$ . However, the vertical plane develops further back from the wall and the sloped section is flatter, in this case. The series of vertical blue cracks in the lower half of the wall suggests that a “toppling” type of failure may initially combine with a subsequent shear failure plane to apply pressure to the cantilever wall.

In the absence of a retaining wall, the pattern of shear planes and cracks develops much closer to the wall face than was observed near the cantilever wall. Although a relatively uniform surcharge pressure was applied to a distance of six feet from the wall, a shear plane developed in the LCC just behind the first surcharge block at a distance of two feet behind the wall. A significant vertical offset is observed across the top of the LCC block in Fig. 12 (a). The shear crack propagates nearly vertically to a depth of about 5 ft (mid-height of the wall), then slopes down to the base of the wall at an angle of  $62^\circ$  from the horizontal as shown in Fig. 11. This failure angle is obviously much steeper than was observed in the LCC behind the cantilever wall.



Fig. 11. Photo showing the blue crack patterns adjacent to the cantilever wall with the six-foot wide surcharge load at the surface. Yellow crack patterns are for a second test with six-foot wide surcharge adjacent to free-face without retaining wall.

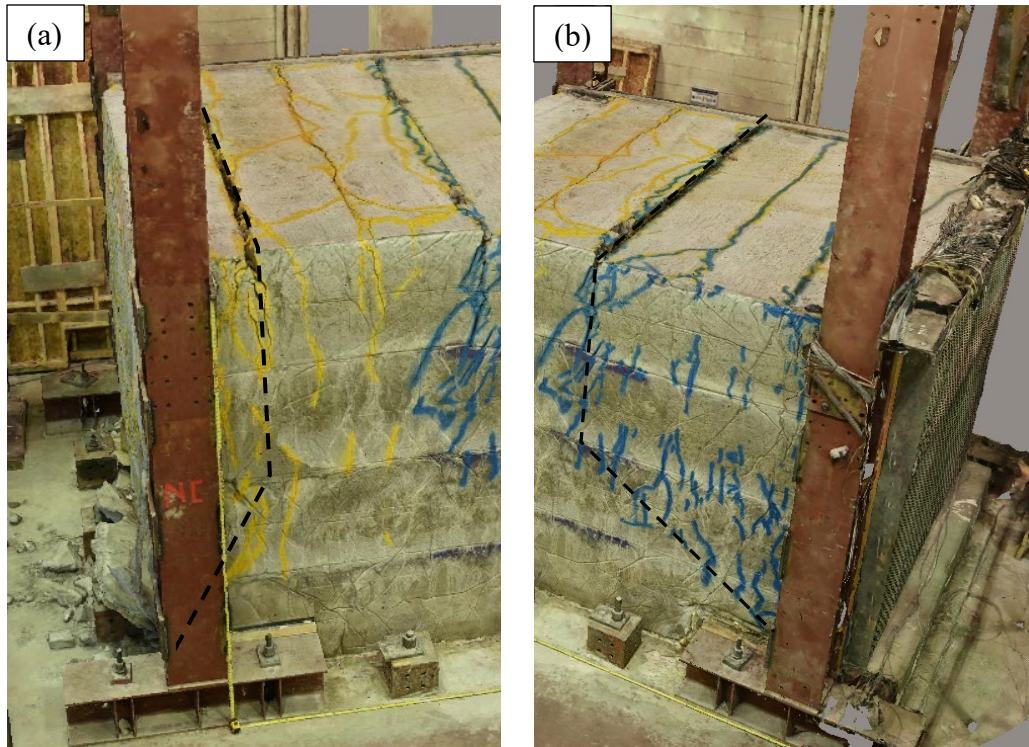


Fig. 12. Three-dimensional point cloud models of (a) crack patterns due to surcharge loading near the free face without a wall and (b) crack patterns due to surcharge loading near the RC retaining wall. (URL for interactive 3D point cloud models)

[http://prismweb11.groups.et.byu.net/CellularTest2\\_Rollins/App/?scene=CellularTest2\\_Rollins&cX=-7.6455&cY=-1.7260&cZ=3.3821&upX=0.0000&upY=0.0000&upZ=1.0000&tX=-1.8247&tY=-1.3051&tZ=0.1494#%2F](http://prismweb11.groups.et.byu.net/CellularTest2_Rollins/App/?scene=CellularTest2_Rollins&cX=-7.6455&cY=-1.7260&cZ=3.3821&upX=0.0000&upY=0.0000&upZ=1.0000&tX=-1.8247&tY=-1.3051&tZ=0.1494#%2F)

If the angle of inclination of the failure slope is assumed to be equal to  $45 + \phi/2$ , as would be the case of an active earth pressure failure, then the back-calculated friction angle is  $34^\circ$ , which is the friction angle that has been recommended for LCC, as discussed previously (Tiwari et al. 2018, Black 2018).

When the wood panel was removed on the back face of the box after completion of the load test on the RC cantilever wall side of the box, no vertical cracks were observed in the free face. This result suggest that the wall was relatively unaffected by the loading on the other side of the box. During the first set of unreinforced LLC tests, when a surcharge was placed over the entire LCC surface, many vertical cracks were observed in the free face. A photograph of the free face at the completion of the surcharge loading adjacent to the free face is shown in Fig. 13. The cracks were spray-painted with yellow paint to highlight their locations. The cracks consist of both vertical and horizontal or inclined cracks. The maximum crack width on one crack was 0.125 inch while the majority are less than 0.06 inch or hairline cracks. There appear to be more cracks in the lower half of the wall than in the top half. Visual observations at the time that the wall was failing indicated that the top half of the wall appeared to be moving as an intact block that was sliding downward on top of the underlying shear planes.



Fig. 13. Photograph of the crack pattern in the LCC on the free face opposite to the cantilever retaining wall side.

### **Preliminary Conclusions**

1. LCC walls can successfully withstand significant surcharge loadings with limited axial and lateral deformations. Failure appears to be relatively ductile when UCS is around 40 psi, but becomes more brittle when UCS is around 100 psi.
2. Surcharging over a limited width (6 feet) produced much more lateral displacement on the RC cantilever retaining wall than a uniform surcharge over the entire surface area for the same pressures. This appears to be a result of the development of shear planes for the limited width loading, but primarily compressive strains for the uniform loading. Failure can occur at surcharge pressures 50 to 60% lower than the UCS.
3. The presence of an RC cantilever retaining wall significantly increased the strength of the LCC block and led to a ductile failure rather than a brittle failure with a loss of strength. This result strongly suggests the wisdom of including a retaining wall in front of an unreinforced LCC.

4. Measured horizontal pressures at the interface between the LCC and cantilever wall at failure were relatively consistent with what would be expected using Rankine earth pressure theory using a friction angle ( $\phi$ ) of  $34^\circ$  and a cohesion of 700 to 1000 psf.
5. Failure surfaces for the free face wall with unreinforced LCC were much steeper and shallower than those supported by an RC cantilever wall. The steep failure surface in the lower half of the wall was generally consistent with a Rankine active earth pressure with a friction angle of  $34^\circ$ .
6. The failure surface for the LCC behind the RC cantilever retaining wall shows a bi-linear shape typical of soil backfill with MSE wall reinforcements that provide an effective cohesion. The composite failure surface is vertical to about 50% of the wall height and then inclines towards the connection between the base slab and stem wall.